Brazilian Journal
of Chemical
Engineering

ISSN 0104-6632
Printed in Brazil
www.abeq.org.br/bjche

Vol. 24, No. 03, pp. 375 - 388, July - September, 2007

NATURAL CONVECTION HEAT TRANSFER IN PARTIALLY OPEN ENCLOSURES CONTAINING AN INTERNAL LOCAL HEAT SOURCE

V. C. Mariani[1*] and L. S. Coelho[2]

[1]Pontifical Catholic University of Paraná, Graduate Program in Mechanical Engineering,
PUCPR/CCET/PPGEM, Imaculada Conceição 1155, CEP: 80215-901, Curitiba PR, Brazil
E-mail: viviana.mariani@pucpr.br
[2]Pontifical Catholic University of Paraná, Graduate Program in Industrial Systems and Engineering,
Automation and Systems Laboratory, PUCPR/CCET/PPGEPS,
Imaculada Conceição 1155, CEP: 80215-901, Curitiba - PR, Brazil.
E-mail: leandro.coelho@pucpr.br

(Received: May 30, 2005 ; Accepted: May 25, 2007)

Abstract - A numerical study was conducted to investigate steady heat transfer and flow phenomena of natural convection of air in enclosures, with three aspect ratios (H/W = 1, 2, and 4), within which there is a local heat source on the bottom wall at three different positions, W_h. This heat source occupies 1% of the total volume of the enclosure. The vertical walls in the enclosures are insulated and there is an opening on the right wall. The natural convection is influenced by the difference in temperature between the left and right walls, represented by a Rayleigh number (Ra_e), and by local heat source, represented by a Rayleigh number (Ra_i). Numerical simulations were performed for several values of the Rayleigh number ranging between 10^3 and 10^6, while the intensity of the two effects – the difference in temperature on the vertical walls and the local heat source – was evaluated based on the Ra_i/Ra_e ratio in the range between 0 and 2500. The analysis proceeds by observing variations in the streamlines and isotherms with respect to the different Ra_e, R ratios, aspect ratios, of the radius and positions of the local heat source. The average Nusselt numbers on the hot and cold walls are influenced by different values of the parameters R, Ra_e, W_h, and H/W. Results show the presence of different flow patterns in the enclosures studied. Thus, the flow and heat transfer can be controlled by external heating, and local heat source.
Keywords: Natural convection; Average Nusselt number; Rectangular enclosures; Numerical study; heat source.

INTRODUCTION

In recent years, numerical modeling of the convective heat transfer problem has been an area of great interest due to its broad applications in engineering. Compared to the experimental method, numerical analysis provides a more direct way to enhance/reduce heat transfer effectively so as to improve the performance or to optimize the structure of a thermal device.

Natural convection in enclosures has been studied both experimentally and numerically, due to the considerable interest in its many engineering applications, such as building insulation, solar energy collection, cooling of heat-generating components in the electrical and nuclear industries, and flows in rooms due to thermal energy sources (Yang, 1987).

Numerical studies of natural convection heat transfer and flow in closed enclosures without a local heat source are reported in the literature; we can cite the work of Davis (1983), Hortmann et al. (1990), Le Quéré (1991), Mohamad (1998), Corcione (2003), and Ben-Nakhi and Chamkha (2006).

*To whom correspondence should be addressed

Other authors have studied the natural convection caused by a heat-generating conducting body located inside an enclosure: Chu and Churchill, 1976; Khalilollahi and Sammakia, 1986; Keyhani et al., 1988; Farouk, 1988; Ho and Chang, 1994; Ha et al., 1999; Deng and Tang, 2002; Oztop et al., 2004; Bazylak et al., 2006.

Numerous studies on natural convection caused only by external heating in partially open enclosures have been conducted by Chan and Tien, 1985; Angirasa et al., 1995; Polat and Bilgen, 2002; Bilgen and Oztop, 2005; Lauriat and Desrayaud, 2006. However, few results have been reported for natural convection caused simultaneously by both external heating in partially open enclosures and an internal local heat sources although problems of this type are frequently important and their study is necessary for understanding the performance of complex natural convection flow and heat transfer.

Indirectly related to the present study, Xia and Zhou (1992) studied a square and partially open enclosure with an internal heat source. These authors change the position on the bottom wall or left vertical wall for only three R ratios. They found that the opening was advantageous to the flow and heat transfer in the cavity. In this case, the characteristics of flow and heat transfer changed with heat source location, external and internal Rayleigh number, and opening size. Reinehr et al. (2002) examined natural convection using the aspect ratio H/W = 2, with an internal heat source whose position was varied only on the bottom wall. In that work, no heat transfer results were reported and a limited number of Ra_e and R ratios were also studied.

The present work is a numerical study of natural convection due to the temperature difference between left and right walls and an internal local heat source in three partially open enclosures, for which few results have been reported in the literature. The enclosures have an opening in the cooled right vertical wall, while the left vertical wall is heated and the upper and lower walls are adiabatic. Natural convection is induced by the difference in temperature between the vertical walls, and it is represented by the Rayleigh number (Ra_e) and by an internal local heat source represented by the Rayleigh number (Ra_i), occupying approximately 1% of the enclosure volume.

The study is conducted numerically under the assumption of steady laminar flow for three different values of both the height-to-width aspect ratio of the enclosure of 1, 2, and 4 and the Rayleigh number based on enclosure height in the range between 10^3 and 10^6. The Ra_i/Ra_e ratio in the range between 0 and 2500 and the internal local heat source position at W_h = 0.25, 0.5, and 0.75 on the bottom wall are evaluated. In this context, the influence on flow patterns, temperature distributions and heat transfer rates is analyzed and discussed.

MATHEMATICAL FORMULATION

To model the flow under study, we use the conservation equations for mass, momentum, and energy for the two-dimensional, steady, and laminar flow. For the moderate temperature difference considered in this work, all the physical properties of the fluid, μ, k, and c_p, are considered constant except density, in the buoyancy term, which obeys the Boussinesq approximation. In the energy conservation equation, we neglect the effects of compressibility and viscous dissipation. Thus, the dimensionless equations that govern the flow are

$$\frac{\partial U}{\partial X}+\frac{\partial V}{\partial Y}=0 \tag{1}$$

$$U\frac{\partial U}{\partial X}+V\frac{\partial U}{\partial Y}=-\frac{\partial P}{\partial X}+\Pr\left(\frac{\partial^2 U}{\partial X^2}+\frac{\partial^2 U}{\partial Y^2}\right) \tag{2}$$

$$U\frac{\partial V}{\partial X}+V\frac{\partial V}{\partial Y}=-\frac{\partial P}{\partial Y}+\Pr\left(\frac{\partial^2 V}{\partial X^2}+\frac{\partial^2 V}{\partial Y^2}\right)+Ra_e\Pr\theta \tag{3}$$

$$U\frac{\partial \theta}{\partial X}+V\frac{\partial \theta}{\partial Y}=\left(\frac{\partial^2 \theta}{\partial X^2}+\frac{\partial^2 \theta}{\partial Y^2}\right)+R \tag{4}$$

Definitions of the dimensionless parameters are listed in the Nomenclature section. The fluid in the interior environment is atmospheric air with the Prandtl number, Pr = 0.71 (air is the working fluid). The Rayleigh number (Ra_e) is represented by the difference in temperature between the vertical walls, $10^3 \le Ra_e \le 10^6$. The intensity of heat produced by the source is represented by the Rayleigh number (Ra_i), which is based on the volumetric heat generation rate. The influence of the intensity of the two Rayleigh numbers is evaluated by means of the equation,

$$R=\frac{Ra_i}{Ra_e} \tag{5}$$

where $0 \le R \le 2500$.

The stream function is defined by the following equations

$$u = \partial\psi/\partial y \tag{6}$$

$$v = -\,\partial\psi/\partial x \tag{7}$$

where the numerical results illustrating the fluid's behavior are presented in terms of the dimensionless stream function,

$$\psi_{\mathrm{dim}} = \frac{\psi}{\alpha} \tag{8}$$

Other physical quantities of interest in the present study are the average Nusselt numbers for the hot and cold walls; these variables are defined respectively as

$$\overline{Nu_h} = -\int_0^H \left.\frac{\partial\theta}{\partial X}\right)_{X=0} dY \tag{9}$$

$$\overline{Nu_c} = -\int_{H/2}^H \left.\frac{\partial\theta}{\partial X}\right)_{X=W} dY \tag{10}$$

The air is studied in three rectangular enclosures with width W and height H heated on the left-hand vertical wall and cooled on the upper half of the right-hand vertical wall. These two walls have a prescribed temperature, while the horizontal walls are adiabatic. Schematic representations of the configurations studied are presented in Fig. 1.

The position W_h = 0.25, 0.5, and 0.75, illustrated in Fig. 1 is the distance from the left lateral wall to the center of the heat source. The internal heat generation source is located on the adiabatic bottom wall at different places and occupies 1% of the total volume of the enclosure. The lower half of the right wall is open and is in contact with the air outside the enclosure. The boundary conditions used are

$$U = V = 0 \text{ and } \theta = 1 \text{ at } X = 0 \text{ and } 0 \le Y \le H \tag{11a}$$

$$U = V = 0 \text{ and } \theta = 0 \text{ at } X = W \text{ and } H/2 \le Y \le H \tag{11b}$$

$$U = V = 0 \text{ and } \partial\theta/\partial Y = 0 \text{ at } 0 \le X \le W \text{ and } Y = 0 \tag{11c}$$

$$U = V = 0 \text{ and } \partial\theta/\partial Y = 0 \text{ at } 0 \le X \le W \text{ and } Y = H \tag{11d}$$

$$K\,\partial\theta_s/\partial n = \partial\theta_f/\partial n \text{ at the source-fluid interfaces} \tag{11e}$$

where K is the ratio of the thermal conductivities between the heated source and the fluid, θ_s is the dimensionless temperature in the heated source, and θ_f is the dimensionless temperature in the fluid. The velocity and temperature profiles for the opening are assumed to be,

$$\partial\theta/\partial X = 0 \text{ if } U > 0 \text{ or else } \theta = 0;\ V = 0 \text{ at } X = W \text{ and } 0 \le Y \le H/2. \tag{12}$$

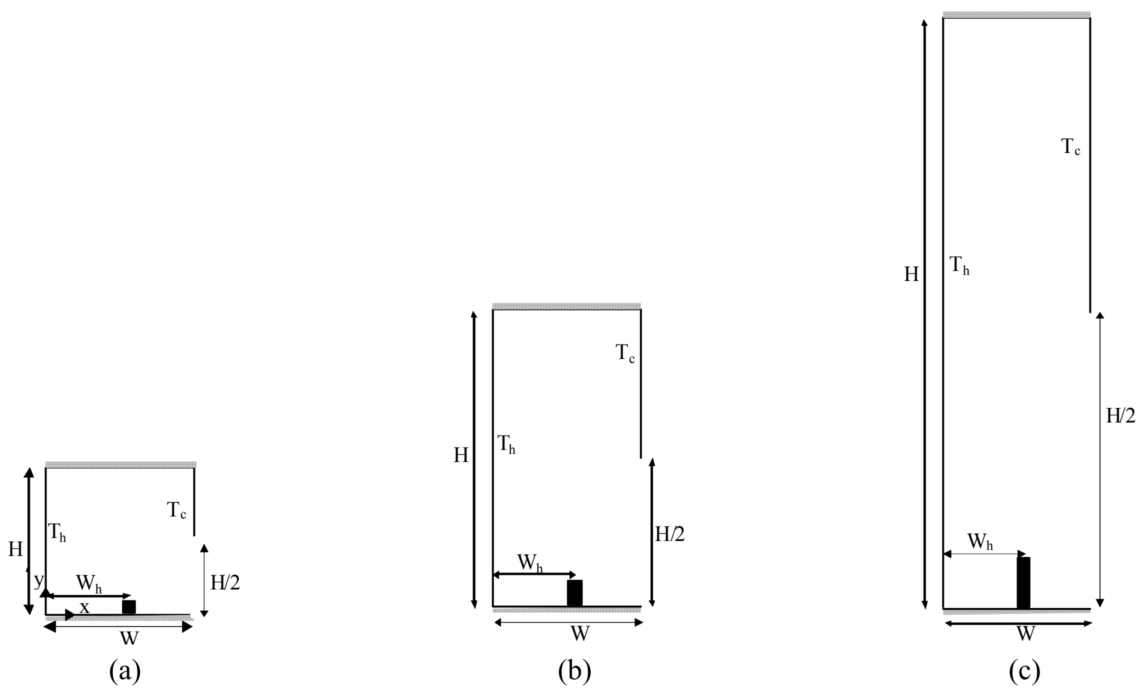

Figure 1: Configurations studied (a) H/W = 1, (b) H/W = 2, and (c) H/W = 4.

SOLUTION PROCEDURE

The differential equations, represented by equations (1) to (4), together with respective boundary conditions, equations (11) and (12), are solved using the finite volume method (MVF) described in Patankar (1980). In this method the solution domain is divided into small finite control volumes. The differential equations are integrated into each of those control volumes. From this integration there were algebraic equations which, when solved simultaneously or separately, supplied pressure and velocity components. A power law scheme is adopted for the convection-diffusion formulation. For the pressure-velocity coupling the SIMPLEC algorithm (semi implicit method for pressure linked equations consistency) is used (Patankar, 1980).

The discretized equations are solved iteratively, using the line-by-line method known as the Thomas algorithm or TDMA (tridiagonal matrix algorithm). An underrelaxation parameter of 0.5 was used in order to obtain a stable convergence for the solution of momentum and energy equations, while there was no need for such a parameter in the solution of the pressure equation.

Validation of the computer code for this work was verified for the natural convection problem in a closed enclosure without a local heat source. The results presented here are for two Rayleigh numbers, $Ra_e = 10^5$ and $Ra_e = 10^6$. Hortman et al. (1990) found the average Nusselt numbers 4.616 and 4.525 for $Ra_e = 10^5$ and grids 42 × 42 and 82 × 82, respectively, while in our study 4.604 and 4.535, respectively, were found. For the $Ra_e = 10^6$ they found the average Nusselt numbers 9.422 and 8.977 for the same grids, while in our study 9.487 and 8.975, respectively, were found.

Grid-independence tests were conducted for all the configurations studied in this work. Three different grid sizes (22 × 22, 42 × 42 and 82 × 82) were used and, for example, for H/W = 1, Ra_e = 2500, and R = 1000 the average Nusselt numbers for the hot wall obtained were -3.87, -4.01, and -4.06 and for the cold wall 4.45, 4.40, and 4.38, respectively, were found for the grids. Because of the small differences for the 42 × 42 and 82 × 82 grids, a 42 × 42 uniform grid was chosen for all the simulations presented in this work. Staggered storage of the variables was used. The numerical solution is considered to be converged when the maximum absolute value of the mass conservation was smaller than 10^{-10}.

NUMERICAL RESULTS AND DISCUSSION

In order to compare the numerical code specifically developed for the present study, some solutions obtained in the square cavity, H/W = 1, when the internal heat source was centrally located at the bottom horizontal wall (at position $W_h = 0.5$) were compared with results of Xia and Zhou (1992) and Reinehr et al. (2002), showing good agreement. These results are presented in Table 1, where different flow patterns occur with the change in Ra_e or R. A comparative analysis between the values in Table 1 shows relative deviation (RD),

$$RD = \left(100.|\Delta\theta_{max}|/\theta_{max}\right)\% \tag{13}$$

where θ_{max} is proposed in Xia and Zhou (1992) and Reinehr et al. (2002) and $\Delta\theta_{max}$ is the difference between the results of this work and those of the two studies mentioned. The results of Xia and Zhou (1992) are situated in the interval of $3.11\% \le \theta_{max} \le 8.3\%$, while for Reinehr et al. (2002) the interval is $0.2\% \le \theta_{max} \le 7\%$, showing good agreement between the results.

Table 1: Maximum dimensionless temperature (θ_{max}) for H/W = 1 and W_h = 0.5.

	Xia and Zhou (1992)	Reinehr et al. (1992)	Present work
R = 400, $Ra_e = 10^5$	1.80	1.82	1.95
R = 1000, $Ra_e = 10^5$	3.90	4.07	4.19
R = 2500, $Ra_e = 10^3$	15.40	15.69	16.08
R = 2500, $Ra_e = 10^4$	10.90	11.50	11.47
R = 2500, $Ra_e = 10^5$	8.30	8.46	8.56
R = 2500, $Ra_e = 10^6$	6.10	-	6.29

According to Table 2 the maximum dimensionless temperature increases considerably with the increasing R ratio, keeping Ra_e constant, independently of the position, heat sources and aspect ratio H/W. The maximum dimensionless temperature decreases with the increasing Ra_e when the R ratio is kept constant. A comparison of the maximum dimensionless temperatures at the same values of R and Ra_e, with the heat source at different positions inside the enclosures indicates that the differences are not significant. When the height of the enclosures increases, the dimensionless temperature also increases, as shown in Table 2.

In Table 3 the dependence of $\overline{Nu_h}$ on R, Ra_e, H/W, and W_h is shown. In the range studied, $\overline{Nu_h}$ undergoes a process from positive to negative with the increasing R for all enclosures studied. When the effect of external heating (Ra_e) on heat transfer in the partially open enclosures is larger than that of the local heat source, $\overline{Nu_h}$ is positive and decreases with increasing R at a given Ra_e, and the hot wall plays a role in heating the fluid in the enclosures, but when Ra_e is smaller, $\overline{Nu_h}$ is negative and $|\overline{Nu_h}|$ increases with R and the hot wall plays a role in cooling the fluid in the enclosures. This behavior was also noted by Xia and Zhou (1992). The $\overline{Nu_h}$ changes with the different positions of local heat source, generally increasing with W_h. The $|\overline{Nu_h}|$ value increases with H/W. It can be observed that the value of Nu_h generally doubles with the increasing of enclosures height from H/W = 1 to H/W = 2 and H/W = 2 to H/W = 4. In Table 4 the dependence of $\overline{Nu_c}$ on R, Ra_e, H/W, and W_h is shown. In the range studied, $\overline{Nu_c}$ increases with R and Ra_e. $\overline{Nu_c}$ is generally larger when the local heat source is closer to the cold wall. When the enclosure height increases, $\overline{Nu_c}$ increases significantly.

Table 2: Maximum dimensionless temperature for H/W = 1, 2, and 4, respectively.

W_h	R	Ra_e 10^3	10^4	10^5	10^6
0.25	400	3.29; 4.39; 5.20	2.66; 3.49; 3.89	2.06; 2.53; 2.84	1.49; 1.83; 2.10
	1000	6.95; 9.39; 10.97	5.56; 7.15; 7.94	4.19; 4.78; 5.55	3.05; 3.49; 4.01
	2500	15.34; 20.77; 23.54	11.97; 14.58; 16.61	8.54; 9.64; 11.36	6.32; 7.22; 8.25
0.5	400	3.50; 4.92; 6.02	2.62; 3.60; 3.89	1.95; 2.47; 2.73	1.36; 1.71; 2.00
	1000	7.64; 10.52; 12.02	5.62; 7.14; 7.74	4.19; 4.77; 5.40	2.97; 3.45; 3.91
	2500	16.08; 21.20; 38.31	11.47; 14.41; 15.99	8.56; 9.68; 11.18	6.29; 7.22; 8.14
0.75	400	3.01; 4.39; 5.37	2.46; 3.72; 3.79	1.86; 2.40; 2.72	1.33; 1.58; 1.95
	1000	7.08; 10.10; 11.19	5.58; 7.16; 7.64	4.13; 4.73; 5.37	2.93; 3.39; 3.88
	2500	15.29; 20.28; 23.24	11.50; 14.33; 15.89	8.48; 9.60; 11.13	6.33; 7.17; 8.11

Table 3: Average Nusselt number on the hot wall for H/W = 1, 2, and 4, respectively.

W_h	R	Ra_e 10^3	10^4	10^5	10^6
0.25	400	-2.14; -4.59; -8.74	-0.94; -1.77; -3.49	1.95; 4.88; 7.33	8.61; 14.81; 23.33
	1000	-6.87;-14.42;-26.74	-5.25;-10.50;-21.02	-1.92; -3.51; -9.40	4.83; 5.87; 8.61
	2500	-18.03;-35.19;-68.5	-15.59;-29.9;-62.48	-11.53;-24.15;-51.9	-4.98;-12.44;-28.48
0.5	400	-1.26; -3.41; -6.39	-0.50; -0.97; -2.28	2.30; 5.35; 8.37	9.13; 14.90; 24.55
	1000	-4.50;-11.09;-20.99	-3.38; -7.85; -18.1	-0.78; -3.46;-9.47	5.69; 8.85; 11.82
	2500	-11.28;-20.27;-55.0	-9.20;-23.17;-55.43	-8.03;-19.97;-44.25	-1.50; -7.07;-19.77
0.75	400	-0.29; -0.85; -2.03	-0.03; -0.29; -0.59	2.47; 5.19; 6.54	9.46; 15.25; 25.11
	1000	-1.82; -6.34;-13.56	-2.06; -5.99; -15.04	-0.27; -2.24; -6.25	5.21; 9.82; 14.38
	2500	-5.89;-16.79;-43.45	-8.67;-18.12;-48.79	-5.49;-15.95;-39.21	-1.15; -4.80; -15.42

Table 4: Average Nusselt number on the cold wall for H/W = 1, 2, and 4, respectively.

W_h	R	Ra_e 10^3	10^4	10^5	10^6
0.25	400	1.27; 2.23; 3.26	2.32; 4.27; 7.09	3.70; 6.52; 11.47	6.83; 12.02; 20.68
	1000	2.22; 3.22; 3.62	3.45; 5.32; 8.11	4.42; 7.39; 12.80	7.28; 12.82; 21.54
	2500	5.13; 6.07; 4.77	6.52; 7.20; 10.39	6.40; 9.95; 17.28	8.64; 14.60; 25.25
0.5	400	1.50; 2.38; 3.39	2.61; 4.58; 7.31	3.79; 6.69; 11.56	6.90; 12.40; 20.70
	1000	3.48; 4.42; 3.95	4.76; 5.91; 8.48	4.80; 8.59; 14.55	7.33; 12.53; 21.65
	2500	9.87; 13.37; 6.21	11.29; 8.32; 11.04	7.53; 11.62; 17.21	8.49; 14.33; 25.69
0.75	400	1.39; 2.06; 3.24	2.55; 4.52; 7.28	3.86; 6.86; 12.39	6.94; 12.20; 20.69
	1000	2.88; 3.33; 3.77	5.30; 6.16; 8.57	5.05; 8.95; 14.12	7.61; 12.54; 21.31
	2500	7.17; 12.51; 5.43	10.97; 9.28; 11.34	8.80; 12.01; 17.99	9.26; 14.42; 25.69

Streamlines and isotherms for R = 2500 are shown in Figs. 2 to 7 for all enclosures and W_h = 0.25, 0.5, and 0.75. An analysis of these figures indicates that when the heating source is located at the center, W_h = 0.5, or close to the opening of the enclosure, W_h = 0.75, various differences occur in the flow pattern according to the change in Ra_e or R. When the local heat source is located at the position W_h = 0.25 close to the hot wall, its influence on the flow patterns and on the heat transfer is negligible.

Verifying the position W_h = 0.5 in Figs. 2 and 3, it can be seen that for $Ra_e = 10^3$ two eddies appear inside the enclosures with H/W = 1 and 2 (see Fig. 2a and 2b) and three eddies appear inside the enclosure with H/W = 4 (see Fig. 2c). They circulate counterclockwise at the left of the enclosure and clockwise at the bottom right, where the intensity of both eddies is important for H/W = 1, i.e., flow and heat transfer are controlled by the internal local heat source and the difference in temperature on the vertical walls has a negligible influence. The left eddy close to the hot wall for H/W = 2 and 4 is less intense than the main flow because the local heat source becomes less important than the difference in temperature between the vertical walls.

In Figs. 4 and 5, for the position W_h = 0.75 it can be seen that at $Ra_e = 10^4$ two main eddies emerge in the enclosure, one circulating counterclockwise close to the hot wall and the other circulating clockwise close to the cold wall. In Figs. 4a and 5a the flow and heat transfer are controlled by the internal local heat source because the intensity of the counterclockwise eddy is much greater than that of the clockwise eddy, while in Figs. 4b, 4c, 5b, and 5c, the flow and heat transfer are controlled by the difference in temperature on the vertical walls.

In Figs. 6 and 7, it can be observed that at W_h = 0.25 for $Ra_e = 10^5$ the enclosures have only a very weak counterclockwise eddy at the backwind side of the local heat source and the larger eddy is a clockwise flow moving upwards along the hot wall and downwards along the cold wall, through the inflow and outflow openings. In these enclosures the flow and heat transfer are controlled by the difference in temperature of the vertical walls.

In Fig. 8 the fluid dynamic behavior of the air in the square enclosure (H/W = 1) is shown. Note that the increase in temperature differences between the vertical walls (Ra_e number) affects the fluid dynamic behavior, increasing the intensity of the flow in the enclosure. This behavior was observed for the various values of R employed, but is illustrated here only for R = 2500 and for the local heat source at the central position on the bottom wall. The main eddy increases with the Ra_e number, although it reaches the full height of the enclosure. In Fig. 9 some of the isotherms obtained for differents Ra_e are shown. Note that the thermal behavior changes as a function of the increasing Ra_e number.

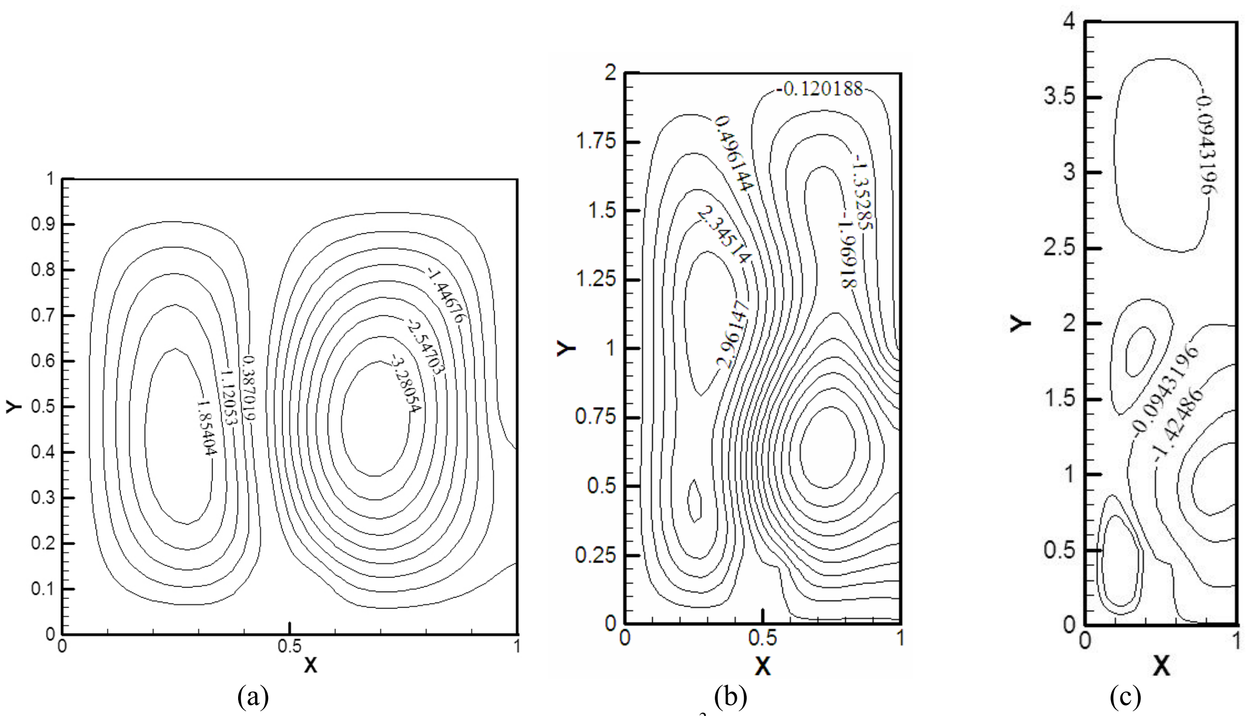

Figure 2: Streamlines for $Ra_e = 10^3$, R = 2500, and W_h = 0.5.

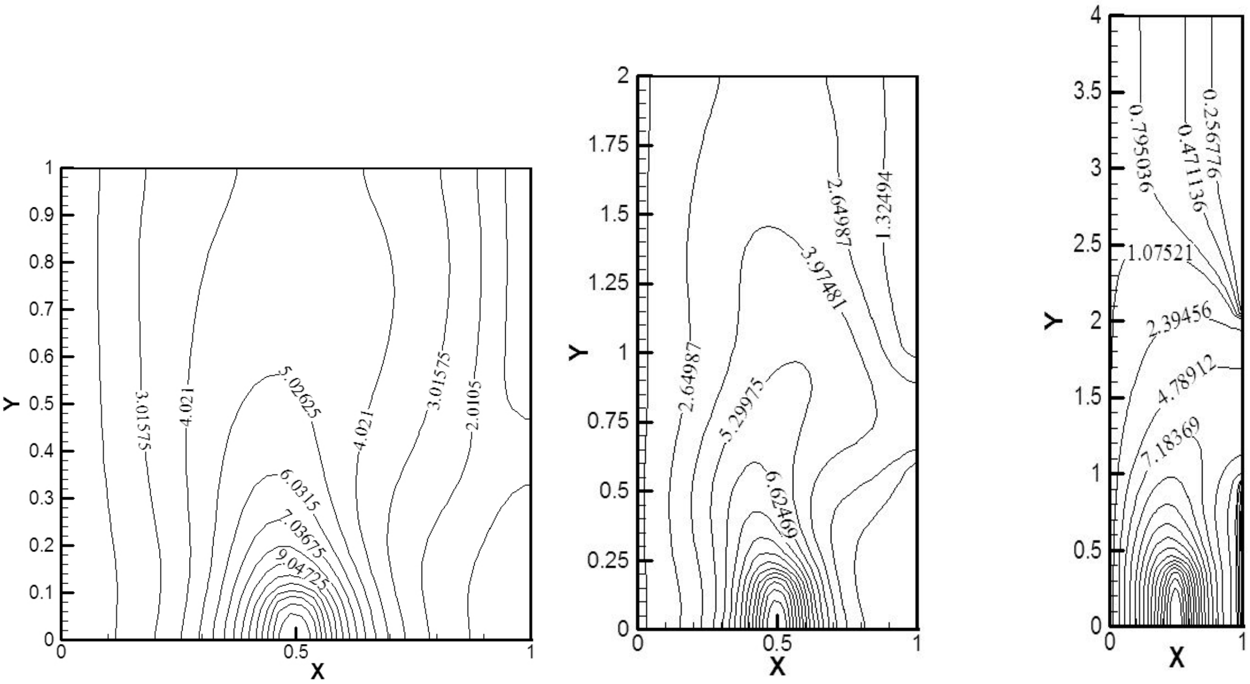

(a) (b) (c)

Figure 3: Isotherms for $Ra_e = 10^3$, R = 2500, and $W_h = 0.5$.

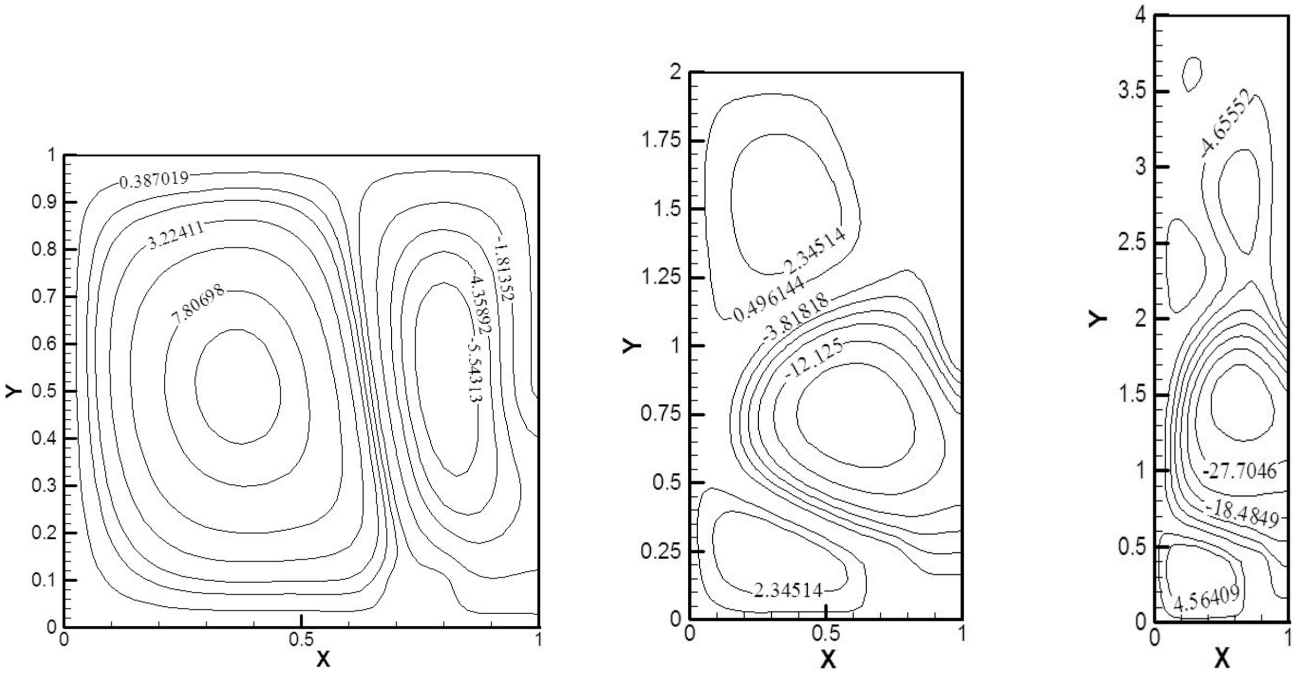

(a) (b) (c)

Figure 4: Streamlines for $Ra_e = 10^4$, R = 2500, and $W_h = 0.75$.

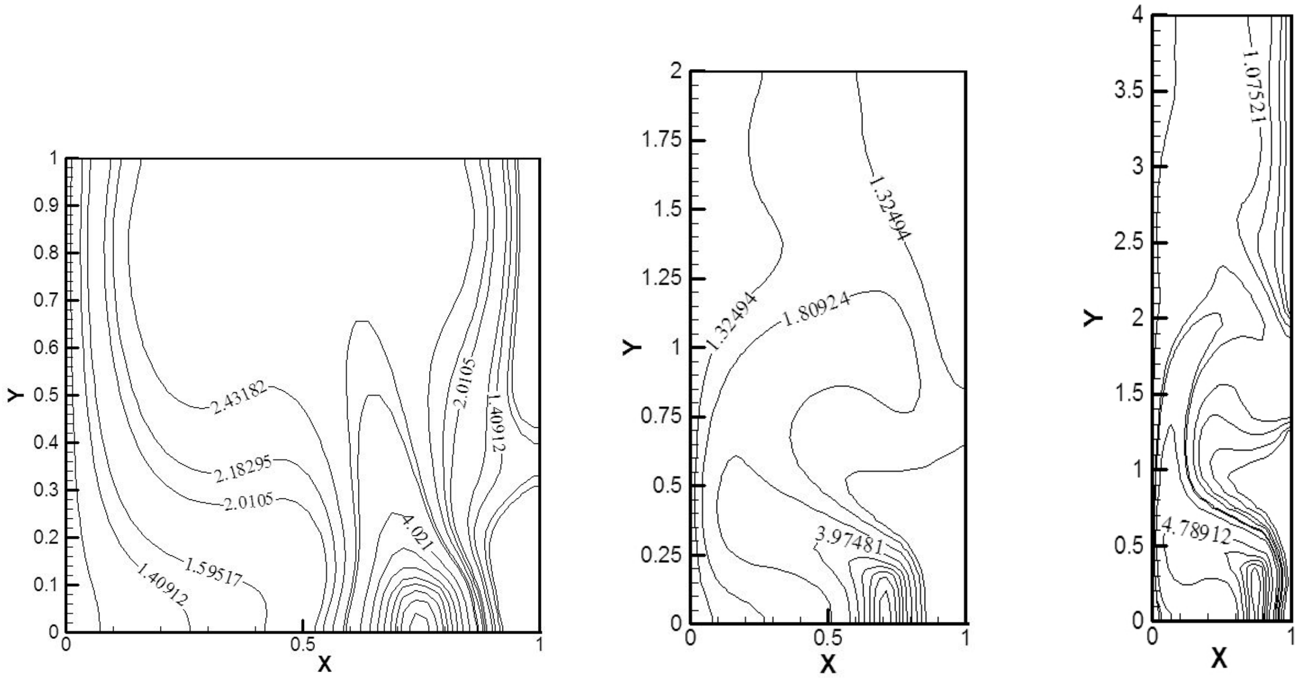

(a) (b) (c)

Figure 5: Isotherms for $Ra_e = 10^4$, $R = 2500$, and $W_h = 0.75$.

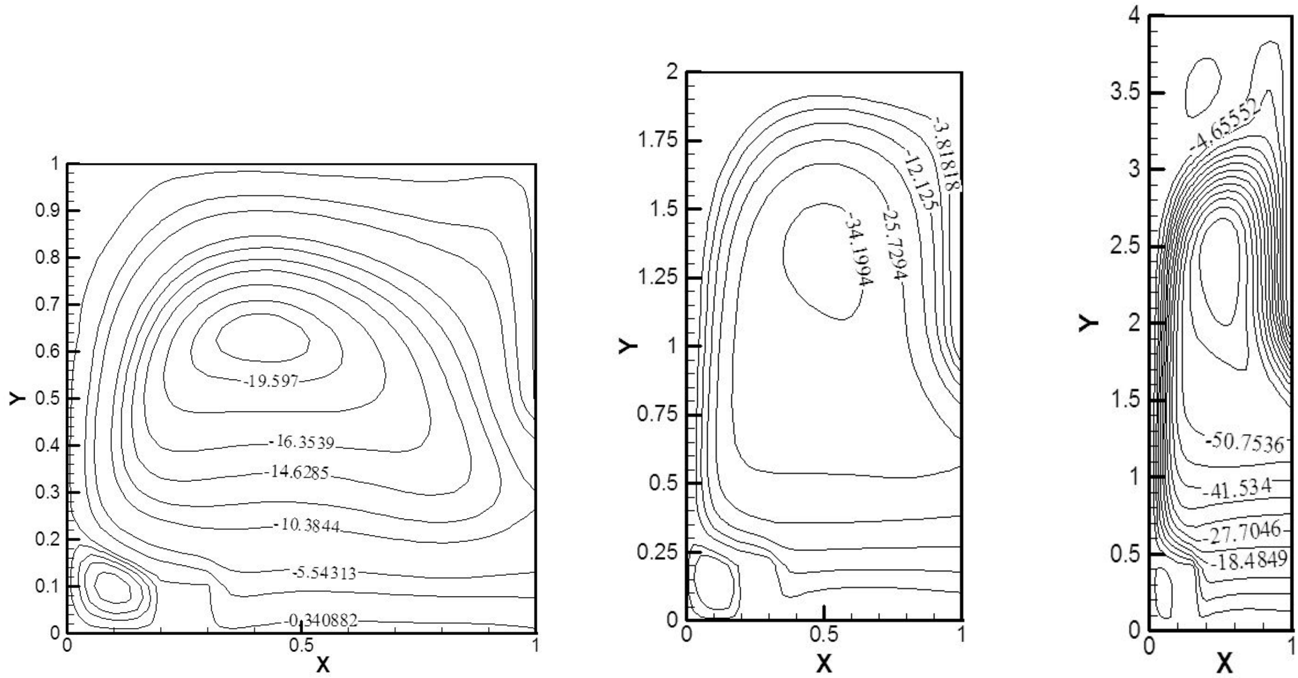

(a) (b) (c)

Figure 6: Streamlines for $Ra_e = 10^5$, $R = 2500$, and $W_h = 0.25$.

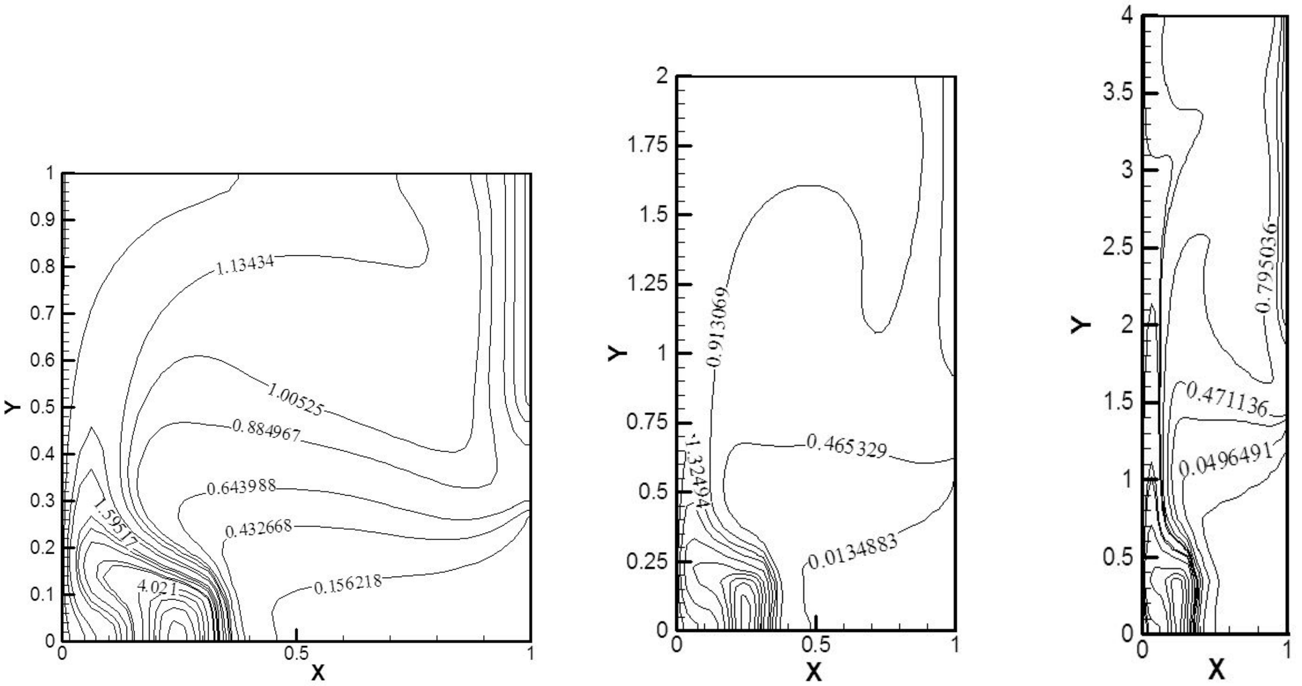

(a) (b) (c)

Figure 7: Isotherms for $Ra_e = 10^5$, R = 2500, and $W_h = 0.25$.

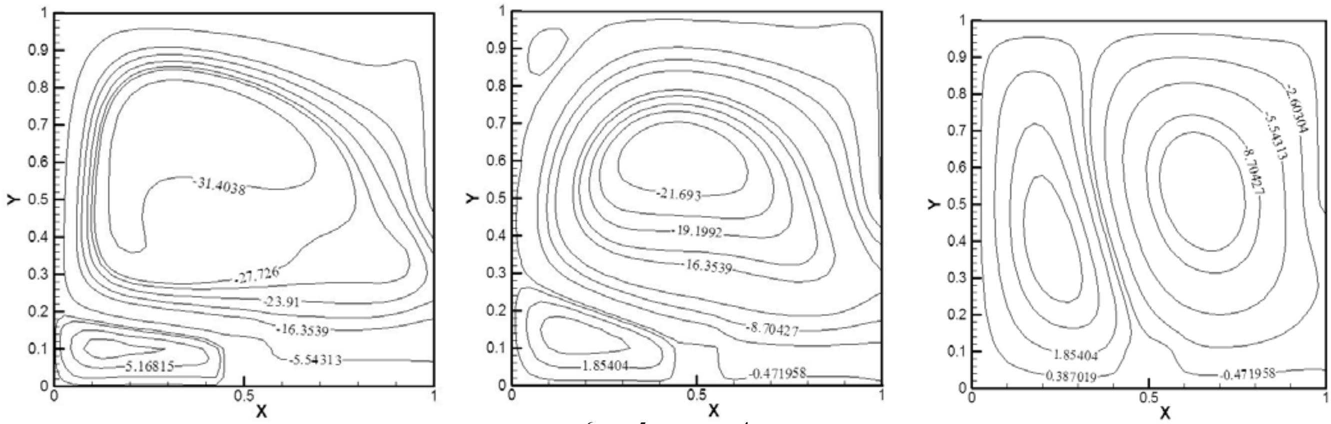

Figure 8: Streamlines for $Ra_e = 10^6$, 10^5, and 10^4; R = 2500, $W_h = 0.5$, and H/W =1.

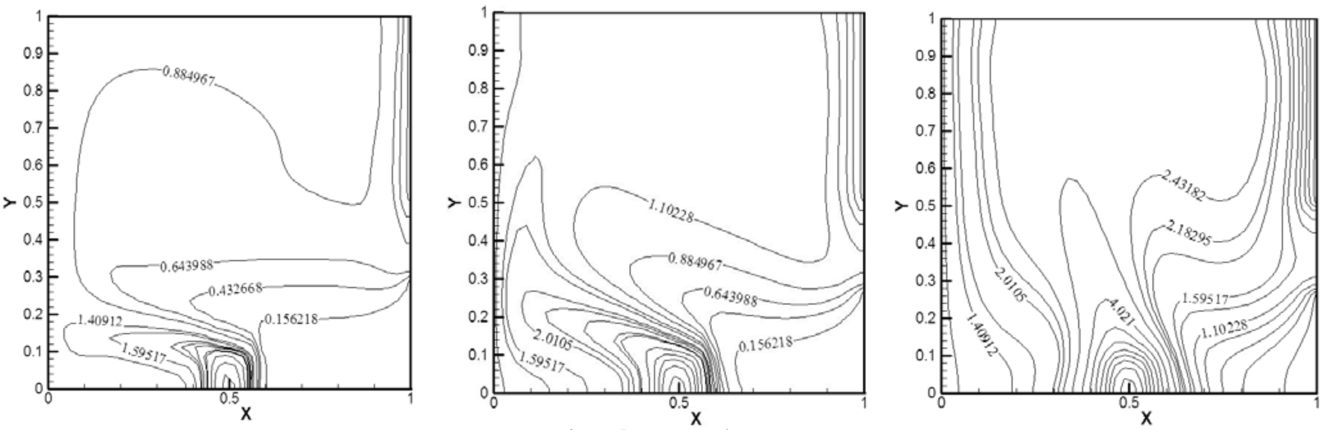

Figure 9: Isotherms for $Ra_e = 10^6$, 10^5, and 10^4; R = 2500, $W_h = 0.5$, and H/W = 1.

The $\overline{\text{Nu}}$ on the hot and cold walls are shown in Figs. 10a, 10b, and 10c, respectively, for H/W = 1, 2, and 4 at $W_h = 0.5$ and R = 2500, as a function of Ra_e. As shown in the isotherms in Fig. 3 and by the dimensionless temperature in Table 2, the fluid temperature decreases with increasing Ra_e for the same R in all enclosures studied in this work. The temperature gradient on the hot wall increases with Ra_e, as shown in Table 3. In this table for approximately R > 400, the $\overline{\text{Nu}_h}$ has negative values, meaning that the fluid temperature next to the hot wall is higher than the hot wall temperature and the heat flow changes direction from the enclosure to the hot wall, while Nu_c increases with Ra_e, meaning that the heat flow from the enclosure to the cold wall increases with this parameter. For example, $\overline{\text{Nu}_c}$ and $\overline{\text{Nu}_h}$ for $Ra_e = 10^5$ are larger than those for $Ra_e = 10^4$ for the same R and all enclosures, due to the increasing convective heat transfer with increasing Ra_e. The dimensionless stream functions ψ_{max} and $|\psi_{min}|$ increase with Ra_e.

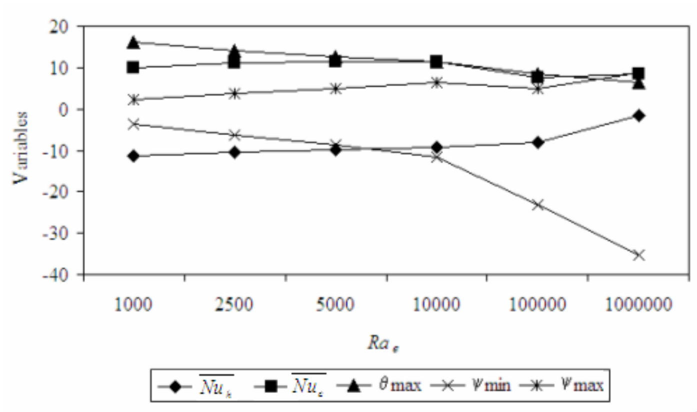

(a)

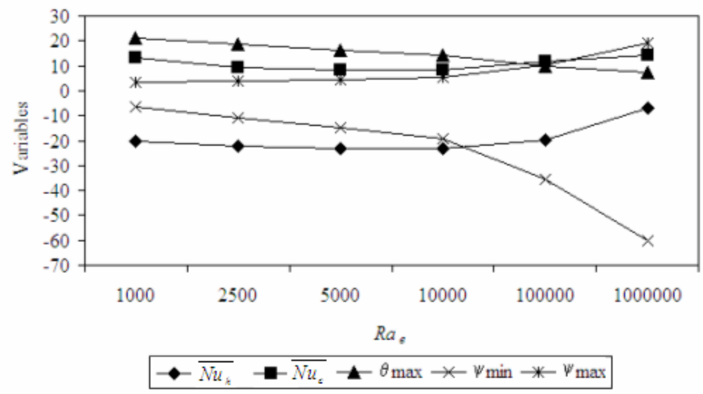

(b)

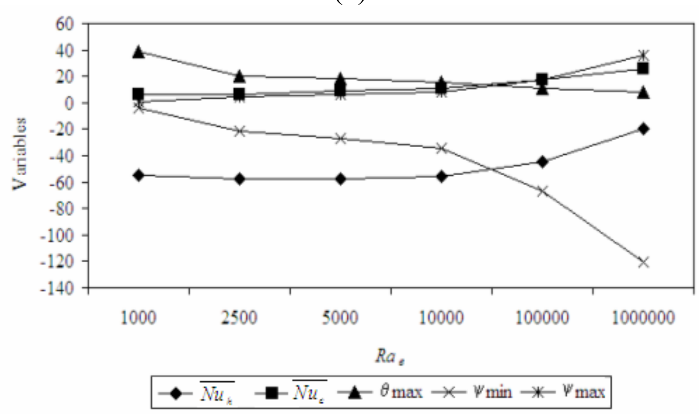

(c)

Figure 10: Effect of Ra_e on various variables with R = 2500, $W_h = 0.5$, and H/W = (a) 1, (b) 2, and (c) 4, respectively.

In Fig. 11 the variation in $\overline{Nu_h}$, $\overline{Nu_c}$, θ_{max}, dimensionless ψ_{max}, and ψ_{min} with the R ratio is shown. In the range studied, the curves are similar, independent of the H/W value; nevertheless the values obtained are different. The $\overline{Nu_c}$ increases with R, meaning that the heat flow from the enclosure to the cold wall increases with this parameter, and on the hot wall, $\overline{Nu_h}$ undergoes a process from positive to negative with increasing R; this effect was shown in the results in Table 3. The dimensionless stream functions ψ_{max} and $|\psi_{min}|$ increase with R. The other variables increase with R for fixed Ra_e. If the effect of external heating on heat transfer in the partially open enclosure is larger than that of the local heat source, then $\overline{Nu_h}$ is positive and decreases with the increasing R at a given Ra_e.

Fig. 12 illustrates the variation in $\overline{Nu_h}$, $\overline{Nu_c}$, θ_{max}, dimensionless ψ_{max}, and ψ_{min} with the location of local heat source for $Ra_e = 10^4$ and R = 1000. For this configuration, when the local heat source moves on the adiabatic wall (bottom wall) small changes in the average Nusselt number and in the other variables occur. When the heat source is located near the opening of the enclosures, the $\overline{Nu_h}$, $\overline{Nu_c}$ (generally) and ψ_{max} values become larger in all enclosures studied. It can be seen in Fig. 12 that the values of all variables are modified smoothly with the change in aspect ratio of all enclosures.

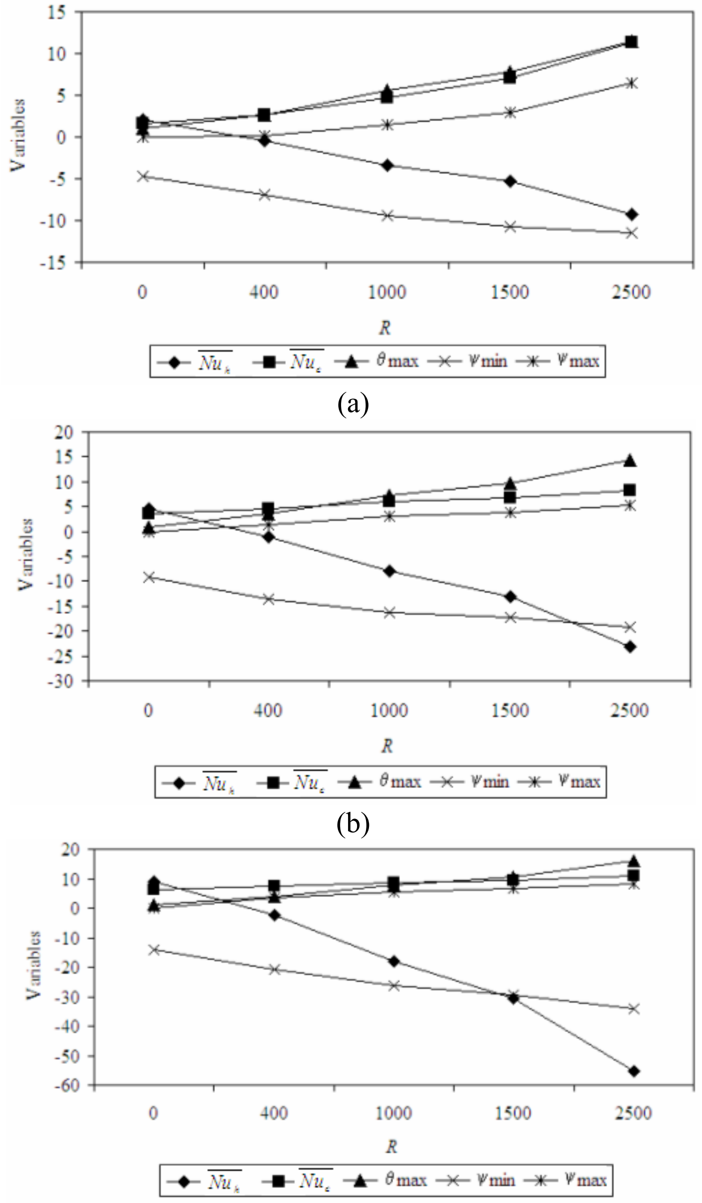

(a)

(b)

(c)

Figure 11: Effect of R on various variables with $Ra_e = 10^4$, $W_h = 0.5$, and H/W = (a) 1, (b) 2, and (c) 4, respectively.

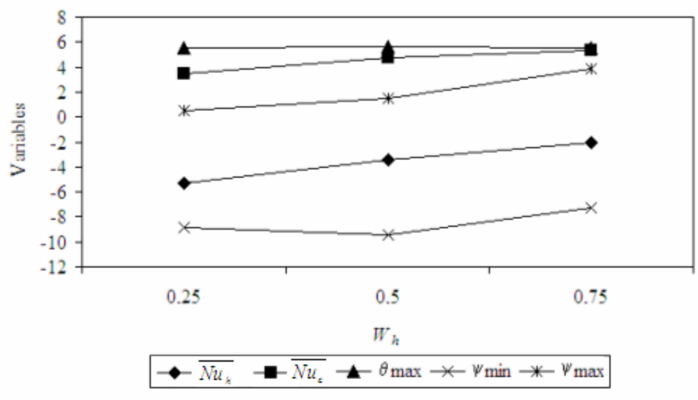

(a)

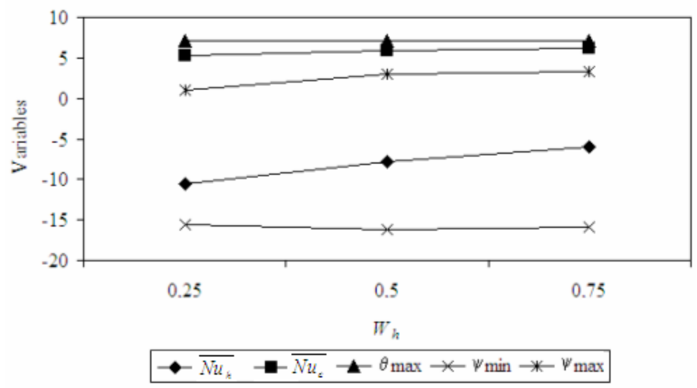

(b)

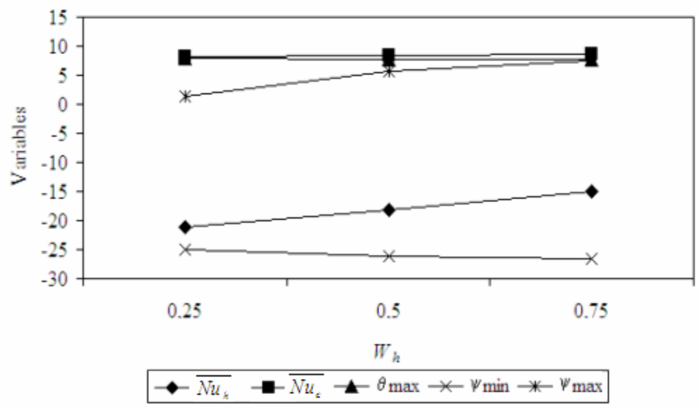

(c)

Figure 12: Effect of location of heat source on various variables with R = 1000, $Ra_e = 10^4$, and H/W = (a) 1, (b) 2, and (c) 4, respectively.

CONCLUSIONS

This work was concerned with the numerical modeling of natural convection in three enclosures, within which there is a local heat source, occupying 1% of the total volume of the enclosures, located on the bottom wall at three different positions. The governing parameters were the Rayleigh number and the R ratio characterizing the heat transfer regime in natural convection. In view of the results, the findings may be summarized as follows:

i) with the increase in Rayleigh number (Ra_e), i. e., in the difference in temperature between the vertical walls, the maximum dimensionless temperature in the internal enclosures decreases, maintaining the R ratio constant, while $\overline{Nu_h}$ and $\overline{Nu_c}$ increase.

ii) with the increase in the R ratio, the maximum dimensionless temperature in the enclosure increases, maintaining the Rayleigh number constant for all positions of the local heat source analyzed, while $\overline{Nu_h}$ decreases and $\overline{Nu_c}$ increases.

iii) the position of the local heat source, W_h, influences the fluid dynamics of the air as well as the heat transfer rate in the enclosures.

iv) the aspect ratio H/W influences meaningfully the results obtained (for example, for maximum dimensionless temperature, small enclosures have lower temperatures, however large enclosures have higher temperatures for the same configurations) for $\overline{Nu_h}$, when the value is positive then it increases and when $\overline{Nu_h}$ is negative it decreases with increasing height of the enclosure, while $\overline{Nu_c}$ increases with increasing height of the enclosure.

v) The opening is advantageous for the flow and heat transfer in the enclosures, and its characteristics are complicated and change with location of internal heat source and external and internal Rayleigh numbers.

NOMENCLATURE

c_p	heat capacity	(J/kg K)
g	acceleration of gravity	(m/s^2)
H	enclosure height	(m)
k	thermal conductivity	(W/m K)
K	ratio of the thermal conductivities between the heated source and the fluid	(-)
$\overline{Nu}$	average Nusselt number	(-)
p	pressure	(Pa)
P	dimensionless pressure	$(= (p + \rho g y)H^3 / \rho\alpha^2)$
P_r	Prandtl number	$(= \nu/\alpha)$
q	rate of local heat generation by the heated protrusion	(W/m^2)
R	Rayleigh number ratio	(-)
Ra_e	external Rayleigh number	$(= (g\beta(T_h - T_c)H^3 / \nu\alpha))$
Ra_i	internal Rayleigh number	$(= (g\beta q H^5 / \nu\alpha k))$
T	temperature	(K)
u	velocity in x direction	(m/s)
v	velocity in y direction	(m/s)
U	dimensionless velocity in x direction	$(= uH/\alpha)$
V	dimensionless velocity in y direction	$(= vH/\alpha)$
W	enclosure width	(m)
W_h	heat generation source location	(m)
x, y	Cartesian coordinates	(m)
X, Y	dimensionless Cartesian coordinates	(= x/H, = y/H)
α	thermal diffusivity	$(= k/\rho c_p)$ (m^2/s)
β	volumetric coefficient of thermal expansion	(K^{-1})
θ	dimensionless temperature	$(=(T-T_c)/(T_h-T_c))$
θ_s	dimensionless temperature in the heated source	(-)
θ_f	dimensionless temperature in the fluid	(-)
μ	dynamic viscosity	(Pa s)
ν	kinematic viscosity	(m^2/s)
ρ	fluid density	(Kg/m^3)
ψ	stream function	(m^2/s)

Subscripts

c	cold	(-)
dim	dimensionless	(-)
e	external	(-)
h	hot	(-)
i	internal	(-)
max	maximum value	(-)
min	minimum value	(-)
w	wall	(-)

REFERENCES

Angirasa, D., Eggels, J. G. M. and Nieuwstadt, F. T. M., Numerical simulation of transient natural convection from an isothermal cavity open on a side, Numerical Heat Transfer, Part A: Applications, Vol. 28, No. 6, pp. 755-768 (1995).

Bazylak, A., Djilali, N. and Sinton, D., Natural convection in an enclosure with distributed heat sources, Numerical Heat Transfer, Part A: Applications, Vol. 49, No. 7, pp. 655-667 (2006).

Ben-Nakhi, A. and Chamkha, A. J., Effect of length and inclination of a thin fin on natural convection in a square enclosure, Numerical Heat Transfer, Part A: Applications, Vol. 50, No. 4, pp. 389-407 (2006).

Bilgen, E. and Oztop, H., Natural convection heat transfer in partially open inclined square cavities, International Journal of Heat and Mass Transfer, Vol. 48, No. 8, pp.1470-1479 (2005).

Chan, Y. L. and Tien, C. L., A numerical study of two-dimensional laminar natural convection in shallow open cavities, International Journal of

Heat Mass Transfer, Vol. 28, No. 3, pp. 603-612 (1985).

Chu, H. H. and Churchill, S. W., The effect of heater size, location, aspect-ratio and boundary conditions on two-dimensional laminar natural convection in rectangular channels, Journal of Heat Transfer, Vol. 98, No. 2, pp. 194-201 (1976).

Corcione, M., Effects of the thermal boundary conditions at the sidewalls upon natural convection in rectangular enclosures heated from below and cooled from above, International Journal of Thermal Sciences, Vol. 42, No. 2, pp. 199-208 (2003).

Davis, G. de V., Natural convection of air in a square cavity: A benchmark solution, International Journal for Numerical Methods in Fluids, Vol. 3, No. 3, pp. 249-264 (1983).

Deng, Q. and Tang, G., Numerical visualization of mass and heat transport for conjugate natural convection/heat conduction by streamline and heatline, International Journal of Heat and Mass Transfer, Vol. 45, No. 11, pp. 2373-2385 (2002).

Farouk, B., Turbulent thermal convection in an enclosure with internal heat generation, Journal of Heat Transfer, Vol. 110, No. 1, pp. 126-132 (1988).

Ha, M. Y., Jung, M. J. and Kim, Y. S., Numerical study on transient heat transfer and fluid flow of natural convection in an enclosure with a heat-generating conducting body, Numerical Heat Transfer, Part A: Applications, Vol. 35, No. 4, pp. 415-433 (1999).

Ho, C. J. and Chang, J. Y., A study of natural convection heat transfer in a vertical rectangular enclosure with two-dimensional discrete heating: Effect of aspect ratio, International Journal of Heat and Mass Transfer, Vol. 37, No. 6, pp. 917-925 (1994).

Hortmann, M., Peric, M. and Scheuerer, G., Finite volume multigrid prediction of laminar natural convection: Benchmark solutions, International Journal for Numerical Methods in Fluids, Vol. 11, No. 2, pp. 189-207 (1990).

Keyhani, M., Prasad, V. and Cox, R., An experimental study of natural convection in a vertical cavity with discrete heat sources, Journal of Heat Transfer, Vol. 100, No. 3, pp. 616-624 (1988).

Khalilollahi, A. and Sammakia, B., Unsteady natural convection generated by a heated surface within an enclosure, Numerical Heat Transfer, Part A: Applications, Vol. 9, No. 6, pp. 715-730 (1986).

Lauriat, G. and Desrayaud, G., Effect of surface radiation on conjugate natural convection in partially open enclosures, International Journal of Thermal Sciences, Vol. 45, No. 4, pp. 335-346 (2006).

Le Quéré, P., Accurate solutions to the square thermally driven cavity at high Rayleigh number, Computers Fluids, Vol. 20, No. 1, pp. 29-41 (1991).

Mohamad, A. A., Benchmark solution for unsteady state CFD problems, Numerical Heat Transfer, Part A: Applications, Vol. 34, No. 6, pp. 653-672 (1998).

Oztop, H. F., Dagtekin, I. and Bahloul, A., Comparison of position of a heated thin plate located in a cavity for natural convection, International Comm. Heat Mass Transfer, Vol. 31, No. 1, pp. 121-132 (2004).

Patankar, S. V., Numerical heat transfer and fluid flow, Hemisphere Washington, D.C. (1980).

Polat, O. and Bilgen, E., Laminar natural convection in inclined open shallow cavities, International Journal of Thermal Sciences, Vol. 41, No. 4, pp. 360-368 (2002).

Reinehr, E. L., Souza, A. A. U. and Souza, S. M. A., Fluid dynamic behavior of air with natural convection and heat generation source in confined environment, In Proceedings of XIV Brazilian Congress of Chemical Engineering, Natal, Rio Grande do Norte, Brazil, pp. 1-8 (2002) (in Portuguese).

Xia, J. L. and Zhou, Z. W., Natural convection in an externally heated partially open cavity with a heated protrusion. FED-vol. 143/HTD, Vol. 232, Measurement and Modeling of Environmental Flows - ASME, Vol. 232, pp. 201-208 (1992).

Yang, K. T., Natural convection in enclosures, in Handbook of Single Phase Convection Heat Transfer, Wiley, New York, NY, USA (1987).